AMERICAN SOCIETY FOR MICROBIOLOGY | Applied and Environmental Microbiology®

BIODEGRADATION

Integrative Analysis of Selected Metabolites and the Fungal Transcriptome during the Developmental Cycle of *Ganoderma lucidum* Strain G0119 Correlates Lignocellulose Degradation with Carbohydrate and Triterpenoid Metabolism

Shuai Zhou,[a,b] Xiaoyu Zhang,[b] Fuying Ma,[b] Shangxian Xie,[b] Chuanhong Tang,[a] Qingjiu Tang,[a] Jingsong Zhang[a]

[a]National Engineering Research Centre of Edible Fungi, Key Laboratory of Applied Mycological Resources and Utilisation, Ministry of Agriculture, Institute of Edible Fungi, Shanghai Academy of Agriculture Sciences, Shanghai, China

[b]Key Laboratory of Biophysics of MOE, College of Life Science and Technology, Huazhong University of Science and Technology, Hubei, China

ABSTRACT To systemically understand the biosynthetic pathways of bioactive substances, including triterpenoids and polysaccharides, in *Ganoderma lucidum*, the correlation between substrate degradation and carbohydrate and triterpenoid metabolism during growth was analyzed by combining changes in metabolite content and changes in related enzyme expression in *G. lucidum* over 5 growth phases. Changes in low-polarity triterpenoid content were correlated with changes in glucose and mannitol contents in fruiting bodies. Additionally, changes in medium-polarity triterpenoid content were correlated with changes in the lignocellulose content of the substrate and with the glucose, trehalose, and mannitol contents of fruiting bodies. Weighted gene coexpression network analysis (WGCNA) indicated that changes in trehalose and polyol contents were related to carbohydrate catabolism and polysaccharide synthesis. Changes in triterpenoid content were related to expression of the carbohydrate catabolic enzymes laccase, cellulase, hemicellulase, and polysaccharide synthase and to the expression of several cytochrome P450 monooxygenases (CYPs). It was concluded that the products of cellulose and hemicellulose degradation participate in polyol, trehalose, and polysaccharide synthesis during initial fruiting body formation. These carbohydrates accumulate in the early phase of fruiting body formation and are utilized when the fruiting bodies mature and a large number of spores are ejected. An increase in carbohydrate metabolism provides additional precursors for the synthesis of triterpenoids.

IMPORTANCE Most studies of *G. lucidum* have focused on its medicinal function and on the mechanism of its activity, whereas the physiological metabolism and synthesis of bioactive substances during the growth of this species have been less studied. Therefore, theoretical guidance for cultivation methods to increase the production of bioactive compounds remains lacking. This study integrated changes in the lignocellulose, carbohydrate, and triterpenoid contents of *G. lucidum* with enzyme expression from transcriptomics data using WGCNA. The findings helped us better understand the connections between substrate utilization and the synthesis of polysaccharides and triterpenoids during the cultivation cycle of *G. lucidum*. The results of WGCNA suggest that the synthesis of triterpenoids can be enhanced not only through regulating the expression of enzymes in the triterpenoid pathway, but also through regulating carbohydrate metabolism and substrate degradation. This study provides a potential approach and identifies enzymes that can be targeted to regulate lignocellulose degradation and accelerate the accumulation of bioactive substances by regulating substrate degradation in *G. lucidum*.

KEYWORDS *Ganoderma lucidum*, lignocellulose, carbohydrate, triterpenoid

Citation Zhou S, Zhang X, Ma F, Xie S, Tang C, Tang Q, Zhang J. 2021. Integrative analysis of selected metabolites and the fungal transcriptome during the developmental cycle of *Ganoderma lucidum* strain G0119 correlates lignocellulose degradation with carbohydrate and triterpenoid metabolism. Appl Environ Microbiol 87:e00533-21. https://doi.org/10.1128/AEM.00533-21.

Editor Isaac Cann, University of Illinois at Urbana-Champaign

Address correspondence to Xiaoyu Zhang, zhangxiaoyuhust@163.com, or Jingsong Zhang, syja16@saas.sh.cn.

Received 15 March 2021
Accepted 14 April 2021
Accepted manuscript posted online 23 April 2021
Published 11 June 2021

Ganoderma lucidum (Curtis) P. Karst, also called Reishi, is a medicinal mushroom that is well known worldwide, especially in Asian countries. The pharmacological activities of *G. lucidum* are widely recognized, as indicated by its inclusion in the *American Herbal Pharmacopoeia* (1). Modern research indicates that *G. lucidum* contains abundant bioactive substances, among which polysaccharides and triterpenoids are of the greatest interest (2). Polysaccharides from *G. lucidum* were found to stimulate spleen cell proliferation, reduce obesity, and modulate gut microbiota (3–5). Triterpenoids inhibit tumor cell growth, induce tumor cell apoptosis, protect the liver, and exert anti-inflammatory effects (6–9). Thus, the demand for *G. lucidum* that produces increased levels of bioactive substances for use either as an herbal medicine or a functional food continues to increase. Most studies have focused on the medicinal functions and mechanisms of these bioactive substances, and the physiological metabolism of substrates and their transformation into carbohydrates and triterpenoids during growth are less well studied. Thus, theoretical guidance related to the cultivation of *G. lucidum* with the goal of producing large amounts of bioactive substances remains insufficient.

Cultivation of *G. lucidum* begins with mycelial colonization of a substrate and the secretion of a series of enzymes that degrade the lignocellulose present in the substrate (10). The degradation products, including monosaccharides and oligosaccharides, are then transported through the mycelium and utilized in several carbohydrate metabolic pathways (11, 12). In basidiomycetes, carbohydrates are metabolized through catabolic pathways, such as the Embden-Meyerhof-Parnas (EMP) pathway and hexose monophosphate (HMP) pathway to supply energy and coenzymes for growth (13–15). Moreover, the metabolites of carbohydrate catabolism are used in the synthesis of other carbohydrates, such as polyol, polysaccharides, and chitin, which function in osmoregulation or carbon storage or act as cell wall components (16, 17). Triterpenoids and sterols are also synthesized from the products of carbohydrate catabolism based on acetyl coenzyme A (acetyl-CoA). In the upstream pathway, the backbones of triterpenoids and sterols are synthesized as lanosterol through the mevalonate (MVA) pathway (18). In the downstream pathway, cytochrome P450 monooxygenases (CYPs) are believed to contribute to the modification of triterpenoids (19, 20). As a large number of metabolites and genes have evolved, the key steps and enzymes that act in the metabolism of triterpenoids are unclear, and our understanding of triterpenoid metabolic regulation in *G. lucidum* is limited.

To obtain *G. lucidum* with increased levels of triterpenoids or polysaccharides, providing sufficient precursors and regulating key steps represent two important solutions. However, how substrate degradation correlates with the synthesis of polysaccharides or triterpenoids and how these metabolic pathways change during growth of *G. lucidum* remain unknown. A study of *Trichoderma reesei* implied a correlation between lignocellulose degradation and carbohydrate metabolism (21). Studies of *Saccharomyces cerevisiae* have revealed a correlation between carbohydrate catabolism and triterpenoid synthesis (22). The relationship between these three metabolic components has rarely been studied. Although recent high-throughput sequencing studies of *G. lucidum* have provided much information about triterpenoid synthesis, carbohydrate synthesis, and wood degradation, the results of these studies are not systemic and do not reveal whether or not these metabolic processes are correlated (23). Additionally, the growth cycle of *G. lucidum* is much longer than those of other filamentous and unicellular fungi, and its metabolite content and gene expression patterns differ at different developmental stages (24, 25). How these metabolic processes interact during growth is also unclear.

In our previous study, we investigated the degradation of lignocellulose, changes in the expression of lignocellulolytic enzymes, and changes in triterpenoid, polysaccharide, and carbohydrate contents during the growth of *G. lucidum* (26–28). In this study, the correlation between lignocellulose degradation and carbohydrate and triterpenoid metabolism during growth suggested by the results of our previous studies was further examined. Compounds whose contents changed in correlation with one another were screened first, and changes in related enzyme expression were then analyzed. By

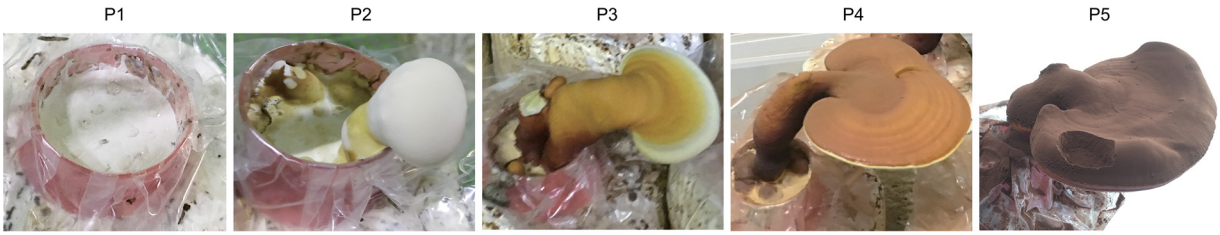

FIG 1 Morphology of *G. lucidum* G0119 at 5 growth phases (P1 to P5). P1, fully grown mycelium (1 month); P2, primordium (2 months); P3, young fruiting bodies (2.5 months); P4, mature fruiting bodies (3.5 months); P5, fully ejected spores (4.5 months).

combining the expression of enzymes that participate in certain metabolic processes and changes in content determined using weighted gene coexpression network analysis (WGCNA), a potential mechanism for this correlation and key enzymes involved in these pathways have emerged.

RESULTS

Changes in lignocellulose, carbohydrate, and triterpenoid contents and their correlation during the growth of *G. lucidum*. The growth cycle was divided into 5 phases for sample testing: P1, fully grown mycelium; P2, primordium; P3, young fruiting bodies; P4, mature fruiting bodies; and P5, fully ejected spores. The morphology of each phase is illustrated in Fig. 1. Changes in the lignin, cellulose and hemicellulose contents of the cultivation substrate are shown in Fig. S1 in the supplemental material. The average lignin content was approximately 22% at P1. From P2 to P4, the lignin content of the three layers decreased significantly. The greatest decrease was observed in the lower layer from P3 to P4 (from 18.74% to 8.51%). From P4 to P5, the lignin content remained low and stable. Both the cellulose and hemicellulose contents decreased similarly during growth. From P1 to P2, there was a significant decrease in the cellulose content of the substrate (from 26.40% to 15.02%), but this occurred primarily in the upper layer and was less evident in the middle and lower layers. There was also a significant decrease in the cellulose content of the lower layer from P3 to P4 (from 21.43% to 9.36%). A significant decrease in the hemicellulose content of the substrate from P1 to P2 was evident only in the upper (from 15.70% to 10.26%) and middle (from 15.08% to 11.52%) layers. A decrease in hemicellulose content from P3 to P4 was clearly evident only in the lower layer (from 14.96% to 5.90%). In general, the lignin, cellulose, and hemicellulose contents of substrate continued to decrease. Approximately 50.67% of the lignin, 40.34% of the cellulose, and 39.25% of the hemicellulose in the substrate were degraded from P1 to P5.

The changes in carbohydrate contents are shown in Fig. S2 in the supplemental material. The primary carbohydrates that accumulated in the substrate and fruiting bodies of *G. lucidum* were glucose, trehalose, arabinitol, and mannitol. The glucose content of the substrate peaked at P1 (1.15 to 1.43%) and decreased from P2 to P3. It then increased to 0.67 to 1%, again from P3 to P4, and decreased at P5. The glucose content of the fruiting bodies continued to increase during growth. From P2 to P3, the glucose content was low (1.86%); it then increased significantly from P4 to P5. The glucose content of the pileus peaked at P5 (18.99%). The trehalose content of the substrate increased from P1 to P3, peaked (in the lower layer) at P3 (0.16%), and then decreased significantly from P3 to P4. From P4 to P5, the trehalose content of the substrate reached its lowest level (0.01 to 0.04%). The trehalose content at the base of the fruiting body peaked at P3 (1.71%) and then decreased to low levels from P4 to P5. The arabinitol content showed a moderate increase throughout the growth cycle. The highest levels of arabinitol (0.40% in the lower layer and 2.02% in the stipe) were detected at P5. The mannitol levels in the substrate increased from P1 to P2, decreased from P2 to P3, and increased again from P3 to P4 before decreasing slightly from P4 to P5. The highest mannitol level (0.11%) was detected in the lower layer at P2. In the fruiting bodies, the mannitol content was high at P2 (4.92%) and then decreased between P2

and P5, except that a high level of mannitol was detected in the pileus at P4 (6.81%). The water-soluble polysaccharide content of the substrate remained stable from P1 to P2 and then increased. The highest observed water-soluble polysaccharide level was 3.16% in the lower layer at P5. Polysaccharide levels in the fruiting bodies were high in the primordium at P2 (2.39%) and then decreased significantly from P2 to P3. From P4 to P5, a moderate increase in polysaccharide levels was observed; at those times, the polysaccharide content was approximately 1.09 to 1.27%.

The changes in triterpenoid content are shown in Fig. S3 in the supplemental material. Reversed-phase high-performance liquid chromatography (RP-HPLC) was used to assess the triterpenoid content. The triterpenoids that eluted earlier were highly polar based on the RP-HPLC elution program. Triterpenoids that eluted before 60 min were designated medium-polarity triterpenoids, and triterpenoids that eluted from 60 to 90 min were designated low-polarity triterpenoids. Generally, medium-polarity triterpenoids accumulated primarily in the primordium, pileus, and stipe. The highest levels of ganoderenic acid B, ganoderic acid B, and ganoderic acid A were all above 1 mg/g and were detected in the stipe at P3. The level of medium-polarity triterpenoid decreased from P2 to P5 and from P3 to P5. Low-polarity triterpenoid levels continued to increase from P2 to P5. The highest levels of ganoderic acid S, ganoderic acid T, and ganoderiol B were detected in the base region at P5 and were all above 1 mg/g.

The data on carbohydrate, triterpenoid, and lignocellulose contents were combined, and the changes in the contents of these compounds during growth were calculated; the Pearson correlation coefficients between the changes of these compounds are shown in Fig. 2. The changes in lignocellulose content over the growth cycle were positively correlated with the changes in trehalose, arabinitol, polysaccharide, and medium-polarity triterpenoid contents in the fruiting bodies. In addition, they were negatively correlated with arabinitol and polysaccharide levels in the substrate, as well as with the levels of glucose and low-polarity triterpenoids in the fruiting bodies. The glucose, arabinitol, mannitol, and polysaccharide contents of the substrate and fruiting bodies generally showed opposite changes. Changes in the content of medium-polarity triterpenoids were inverse to changes the low-polarity triterpenoid content. The above results indicate that when lignocellulose was degraded during growth, the levels of glucose, trehalose, and mannitol in the substrate decreased, and those of arabinitol increased. In the fruiting bodies, polysaccharide and medium-polarity triterpenoid levels decreased, and low-polarity triterpenoid levels increased.

Changes in the expression of genes related to lignocellulose degradation and carbohydrate and triterpenoid metabolism during the growth of *G. lucidum*. The enzymes involved in the metabolism of the compounds detected above were selected from the *G. lucidum* G0119 genome. These enzymes included 32 lignin-modifying enzymes, 36 cellulases, 32 hemicellulases, 58 carbohydrate catabolism enzymes, 55 carbohydrate synthesis enzymes, and 19 enzymes involved in triterpenoid synthesis pathways. They were selected with reference to a book on fungi and lignocellulosic biomass (29) and to KEGG pathway maps (map00010, map00020, map00030, map00500, map00051, map00040, map00100, and map00900). The gene IDs of the genes encoding these enzymes are listed in Table S1 in the supplemental material. Additionally, 167 CYPs were identified as potential candidates for enzymes involved in triterpenoid downstream pathways. The gene IDs of the CYPs are listed in Table S2 in the supplemental material.

The observed changes in the expression of lignocellulolytic enzymes (Fig. 3) indicate that lignin-modifying enzymes and hemicellulases were more highly expressed at P1 and P5 than at other phases. A total of 4 lignin-modifying peroxidases, 2 glyoxal oxidases, 1 β-galactosidase, and 2 endo-1,4-β-xylanases were downregulated by 2.23- to 5.53-fold from P1 to P2. From P2 to P3, the expression of cellulase was upregulated, and a group of 2 β-glucosidases and 1 other β-glucosidase showed increases in expression ranging from 2.90-fold to 4.51-fold. From P4 to P5, most cellulases, several lignin-modifying enzymes, and the hemicellulases were upregulated. A total of 3 lignin-modifying peroxidases, 1 glyoxal oxidase, 2 endo-1,4-β-xylanases, 2 xyloglucan-specific endo-β-1,4-glucanases,

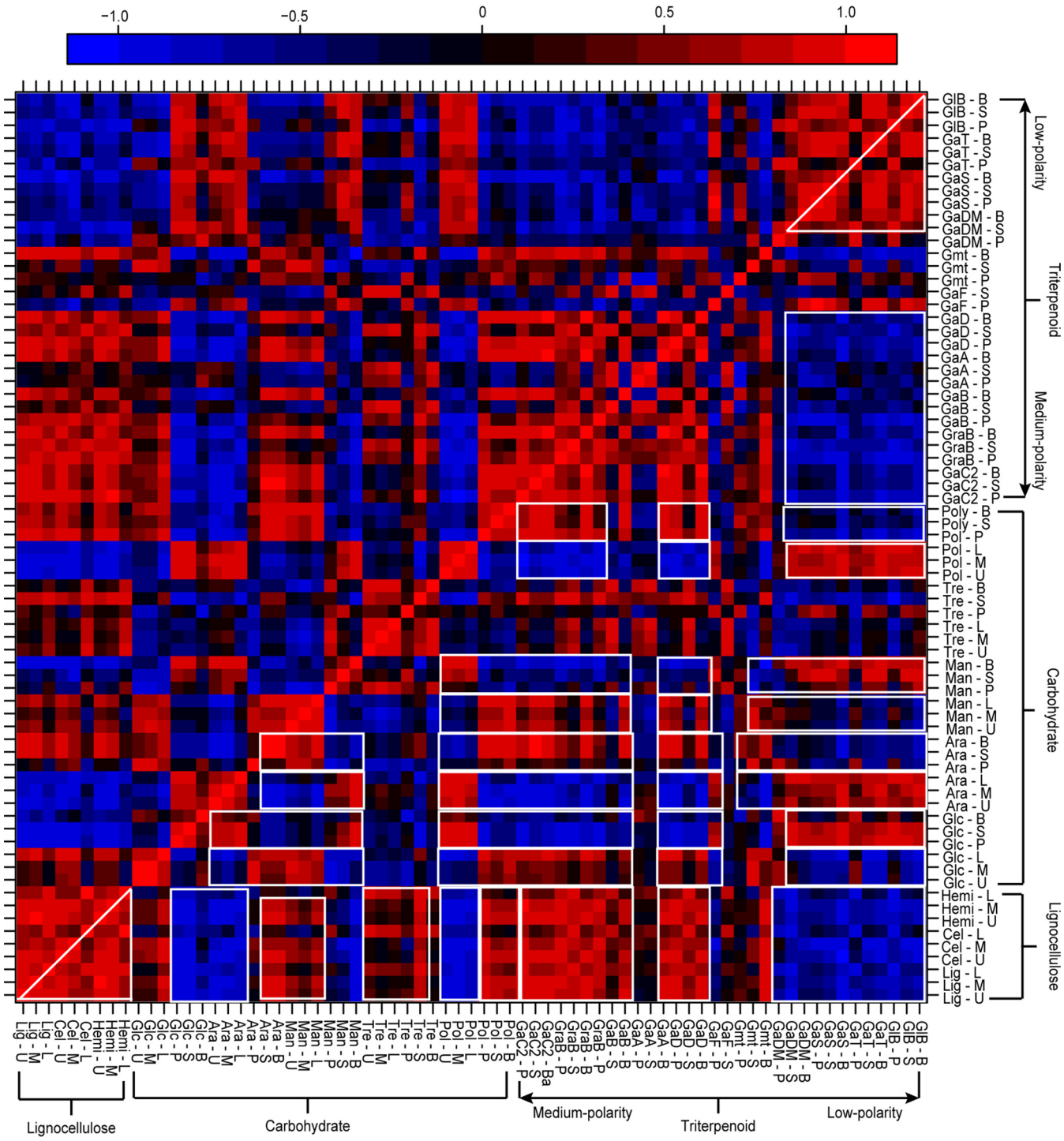

FIG 2 Pearson correlation coefficients for changes in the lignocellulose, carbohydrate, and triterpenoid contents of *G. lucidum* during five phases of growth. Red dots indicate positive correlations, and blue dots indicate negative correlations. White outlines indicate regions of positive and negative correlation. Abbreviations: U, upper layer of the substrate; M, middle layer of the substrate; L, lower layer of the substrate; P, pileus; S, stipe; B, base; Lig, lignin; Cel, cellulose; Hemi, hemicellulose; Glc, glucose; Ara, arabinitol; Man, mannitol; Tre, trehalose; Pol, polysaccharide; GaC2, ganoderic acid C2; GraB, ganoderenic acid B; GaB, ganoderic acid B; GaA, ganoderic acid A; GaD, ganoderic acid D; GaF, ganoderic acid F; Gmt, ganodermanontriol; GaDM, ganoderic acid DM; GaS, ganoderic acid S; GaT, ganoderic acid T; GlB, ganoderiol B.

5 endo-β-1,4-glucanases, 3 cellobiohydrolases, and 3 endoglucanases showed increases in expression of 2.59- to 6.60-fold. These results indicate that the expression levels of lignin-modifying enzymes and hemicellulases decreased from the fully grown mycelium phase to the primordium phase. The expression levels of cellulases increased from the

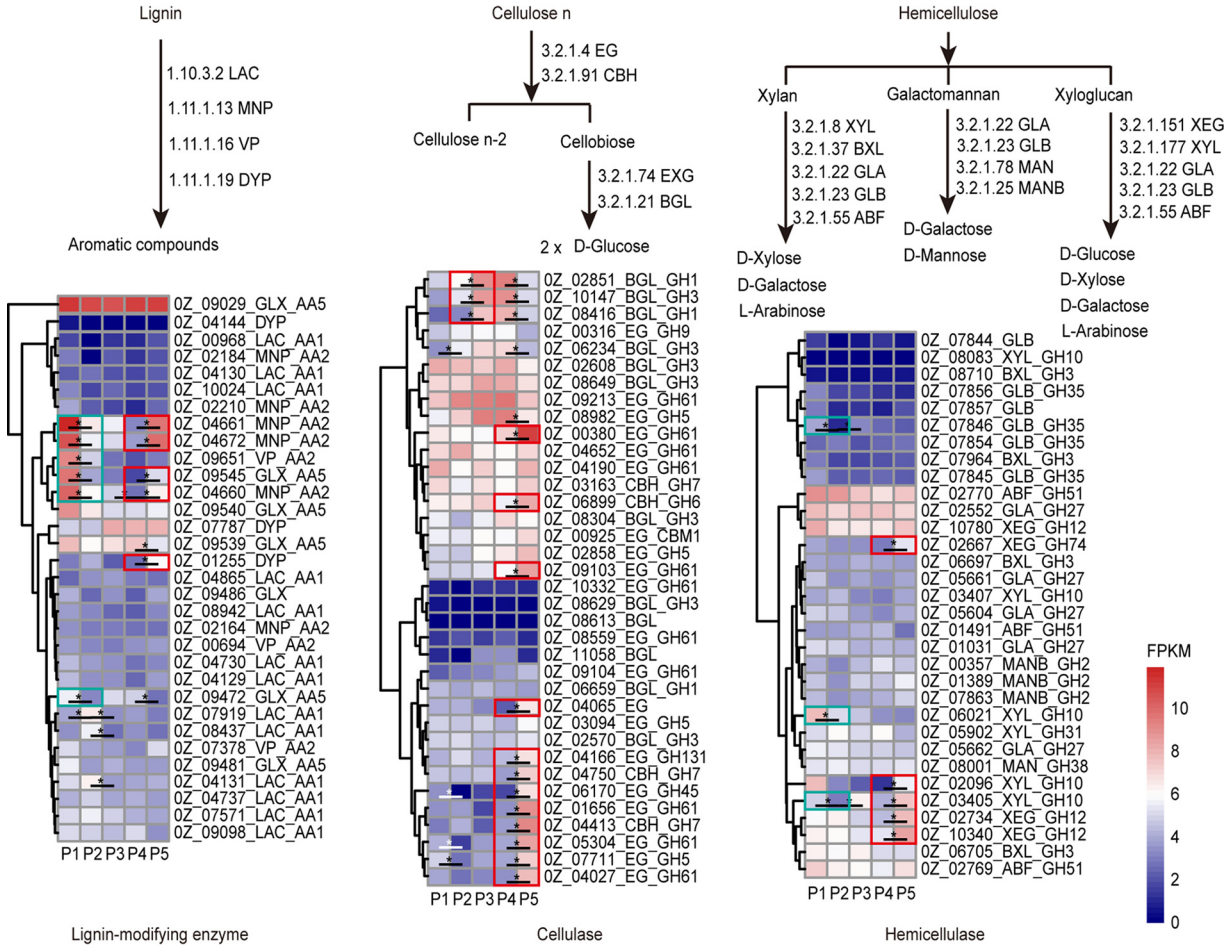

FIG 3 Changes in the expression of lignocellulolytic enzymes in *G. lucidum* during the 5 phases of its growth (P1 to P5). Values that differ significantly (fold change greater than 2 and $P < 0.05$) are marked with black asterisks. Areas outlined in green indicate that the expression of lignin-modifying enzymes and hemicellulase decreased by more than 2-fold from P1 to P2. Areas outlined in red indicate that the expression of cellulase was upregulated by more than 2-fold from P2 to P3. From P4 to P5, most cellulases, several lignin-modifying enzymes, and hemicellulases were upregulated by more than 2-fold.

primordium phase to the young fruiting body phase. From the mature fruiting body phase to the spore-ejecting phase, the expression levels of lignin-modifying enzymes, cellulases, and hemicellulases increased.

The observed changes in the expression of enzymes involved in carbohydrate metabolism are shown in Fig. 4. From P1 to P2, the expression of 1 EMP pathway enzyme and 2 HMP pathway enzymes increased by 2.81-fold and 2.18- to 4.18-fold, respectively. Moreover, 1 enzyme involved in arabinitol metabolism and 1 enzyme involved in mannitol metabolism were also upregulated by 2.41- and 4.18-fold, respectively. The expression of EMP and HMP pathway enzymes subsequently remained high from P2 to P3. During this period, the expression of trehalose metabolism-related enzymes continued to increase. Additionally, the expression of 1 polysaccharide synthase increased by 2.97-fold. From P4 to P5, the expression levels of 3 EMP pathway enzymes, 1 HMP pathway enzyme, and 1 tricarboxylic acid (TCA) pathway enzyme decreased by 2.98- to 3.22-, 3.68-, and 2.80-fold, respectively. In addition, the expression of 4 trehalose metabolism-related enzymes and 1 polysaccharide synthase decreased by 2.16- to 2.67-fold and 3.32-fold, respectively. These results indicated that the synthesis of polyol, trehalose, and glycogen increased during the first half of the growth cycle but decreased in the second half of the growth cycle and that the levels

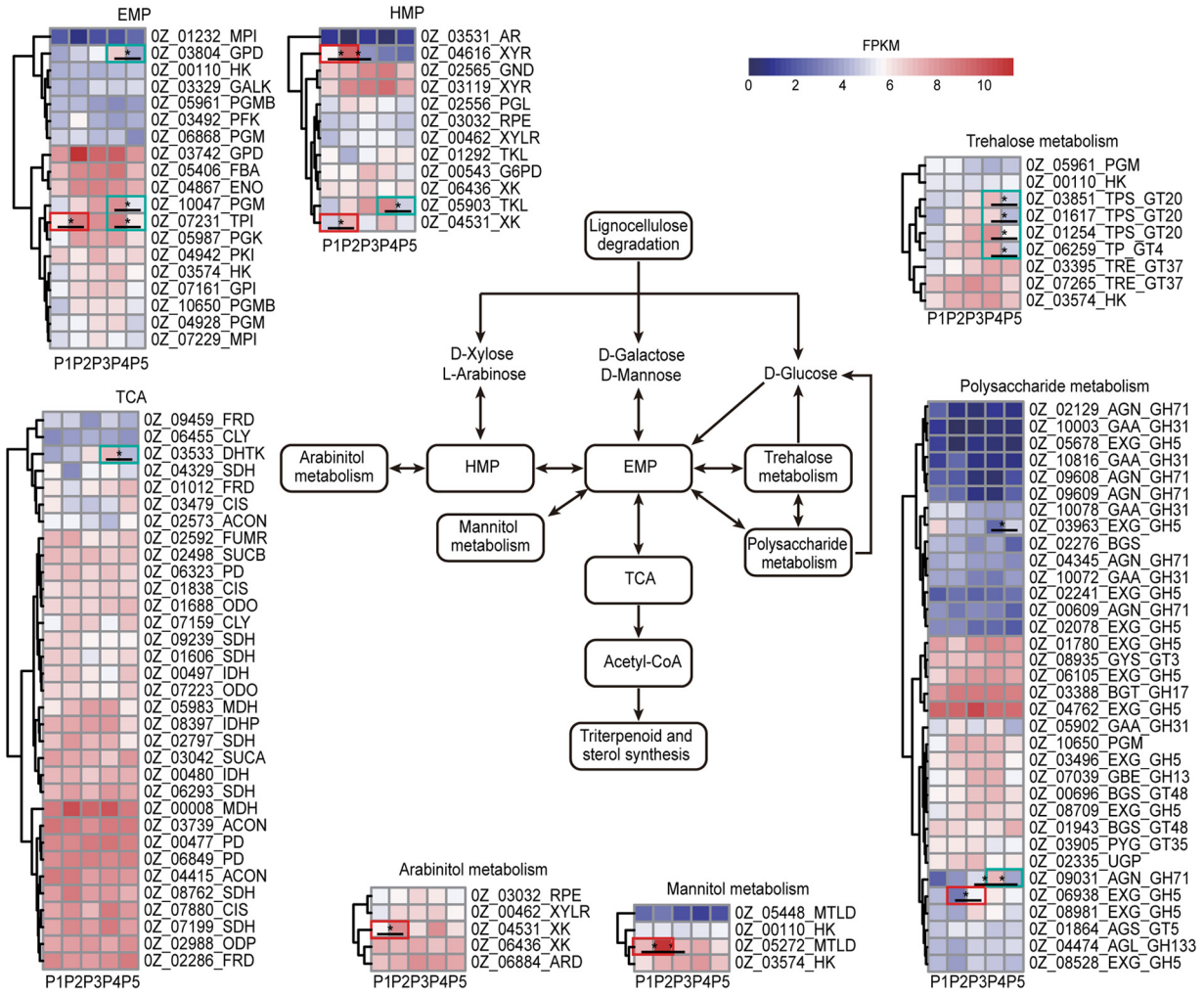

FIG 4 Changes in the expression of genes involved in carbohydrate catabolism in *G. lucidum* during the 5 phases of its growth (P1 to P5). Values that differ significantly (fold change greater than 2 and $P < 0.05$) are marked with black asterisks. Areas outlined in red indicate that the expression levels of EMP, HMP, and TCA pathway enzymes, as well as those of arabinitol, mannitol, trehalose, and polysaccharide metabolic enzymes, increased by more than 2-fold from P1 to P2 and from P2 to P3. Areas outlined in green indicate that the expression levels of EMP, HMP, and TCA pathway enzymes, as well as those of arabinitol, mannitol, trehalose, and polysaccharide metabolic enzymes, decreased by more than 2-fold from P4 to P5.

of expression of carbohydrate catabolism-related enzymes changed with changes in the metabolism of these carbohydrates.

Among the enzymes that act upstream of triterpenoid synthesis, the genes coding for acetyl-CoA acetyltransferase (ACAT), hydroxymethylglutaryl-CoA synthase (HMGS), 3-hydroxy-4-methylglutaryl-CoA reductase (HMGR), and CYP505 were expressed at higher levels than other genes during the growth cycle. Most synthases upstream of triterpenoids, including ACAT, HMGS, HMGR, CYP505, pyrophosphomevalonate decarboxylase (MVD), isopentenyl-diphosphate isomerase (IDI), squalene synthase (SE), and lanosterol synthase (LS), were more highly expressed at P2 and P5 than at other phases, and this coincided with the observed changes in medium-polarity triterpenoid and low-polarity triterpenoid contents (Fig. 5). Additionally, among the CYPs that potentially act downstream of triterpenoid synthesis, the expression levels of 4 CYPs (0Z_01575, 0Z_05924, 0Z_06044, and 0Z_10216) and 3 CYPs (0Z_03686, 0Z_07601, and 0Z_09389) were found to be positively and negatively correlated, respectively, with the expression of LS, with Pearson correlation coefficients above 0.9 (Table S2). As LS

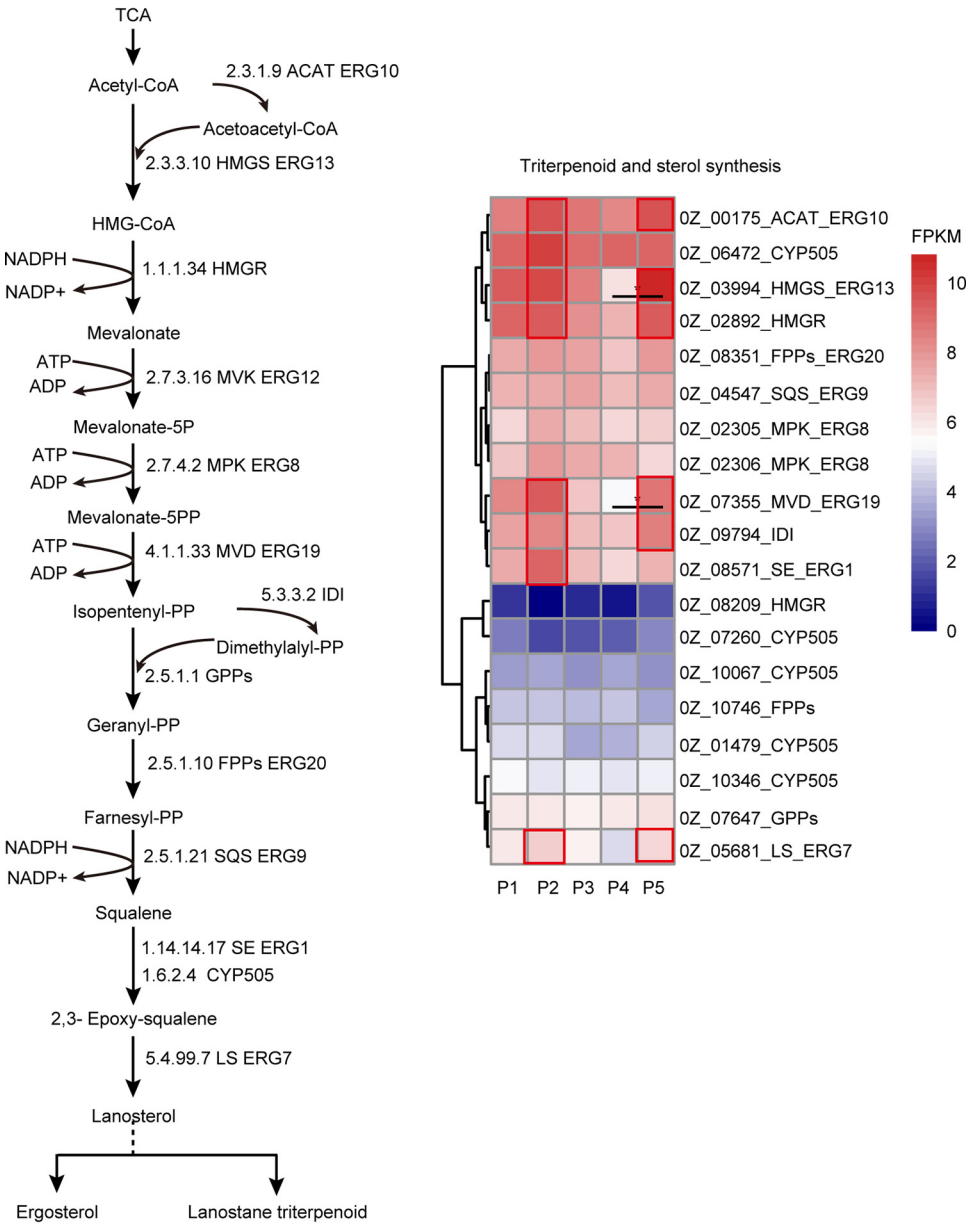

FIG 5 Changes in the expression of genes involved in triterpenoid and sterol metabolism in *G. lucidum* during the 5 phases of its growth (P1 to P5). Values that differ significantly (fold change greater than 2 and $P < 0.05$) are marked with black asterisks. Areas outlined in red indicate that the expression levels of ACAT, HMGS, HMGR, CYP505, MVD, IDI, SE, and LS peaked at P2 and P5.

catalyzes the synthesis of lanosterol in the triterpenoid precursor synthesis, these enzymes might participate in the next step of lanosterol metabolism.

WGCNA of gene expression and changes in the lignocellulose, carbohydrate, and triterpenoid contents of *G. lucidum*. The correlation between gene expression and changes in the content of lignocellulose, carbohydrate, and triterpenoids was studied by WGCNA of related enzymes. The levels of expression of lignocellulolytic enzyme genes, genes related to carbohydrate metabolism and triterpenoid precursor synthesis, CYP genes, and differentially expressed genes (DEGs) in adjacent growth phases were analyzed together.

The genes of interest were divided into 6 modules that are marked with different colors (brown, cyan, green, yellow, blue, and red) based on the similarity of their expression (Fig. 6A). The changes in the content of specific compounds were compared with the

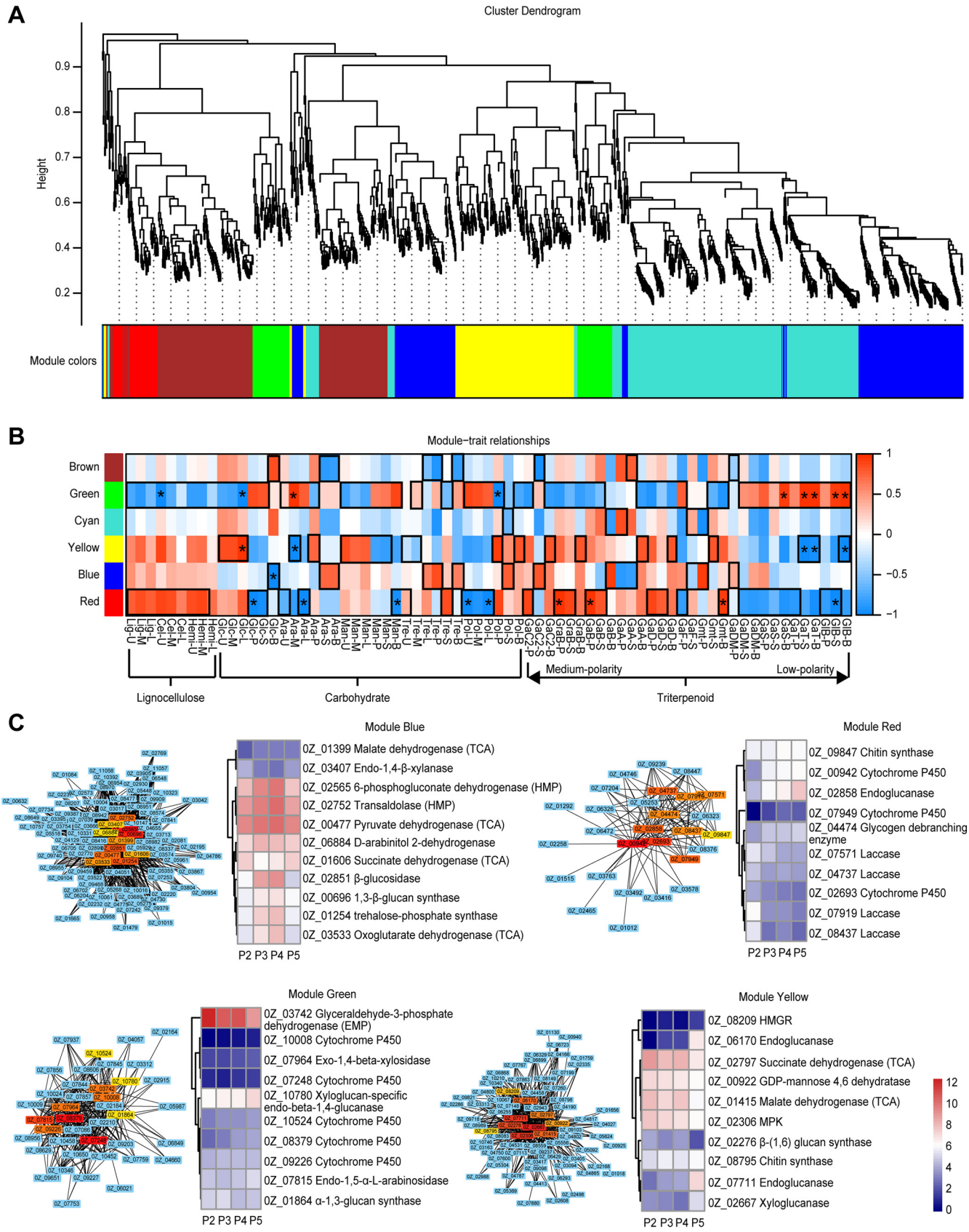

FIG 6 WGCNA changes in gene expression and content of lignocellulose, carbohydrates, and triterpenoids in *G. lucidum*. (A) Dendrogram of modules indicated with different colors. (B) Module-trait relationships between content and gene expression changes. Areas outlined in black indicate metabolites

(Continued on next page)

changes in the expression of the genes in each module by evaluating the correlation values and the *P* values (Fig. 6B). The observed changes in lignocellulose content were most closely correlated with changes in the expression of the genes in the red and green modules. The change in glucose content was most closely correlated with changes in the expression of genes in the green, red, and yellow modules. Arabinitol content was most closely correlated with the expression of genes in the green, red, yellow, and blue modules. Trehalose content was most closely correlated with the expression of genes in the blue and brown modules. Polysaccharide content was most closely correlated with the expression of genes in the green, yellow, and red modules. Medium-polarity triterpenoid content was most closely correlated with the expression of genes in the yellow, green, and red modules. Low-polarity triterpenoid content was correlated with the expression of genes in the green and yellow modules. Genes with correlation *P* values lower than 0.05 were distributed in the red, yellow, blue, and green modules. A coexpression network for each of the 4 modules was constructed and used to evaluate the hub genes. The top 10 genes in each module (ranked by connection degree) were identified as hub genes. The functions of these genes and the observed changes in their expression are shown in Fig. 6C. The hub genes in the red module indicate that changes in medium-polarity triterpenoid content may be correlated with the metabolism of glycogen and chitin and the expression of laccase. The expression of 1 CYP was positively correlated with changes in medium-polarity triterpenoid levels. The hub genes in the yellow module indicate that accumulation of medium-polarity triterpenoids is also correlated with the degradation of cellulose, metabolism of the TCA pathway, and the synthesis of polysaccharides. The hub genes in the blue module indicate that changes in arabinitol and trehalose levels correlate with the degradation of cellulose and hemicellulose and with the HMP and TCA pathways. The hub genes in the green module indicate that the accumulation of low-polarity triterpenoids correlates with the expression of cellulase, hemicellulase, and enzymes involved in glycogen synthesis and EMP metabolism. The expression of 3 CYPs correlated positively with changes in low-polarity triterpenoid content.

DISCUSSION

The results presented above suggest that after cellulose and hemicellulose are degraded, the glucose content of *G. lucidum* increases when the mycelium is fully grown, and as the primary degradation product of cellulose, glucose is then converted into other carbohydrates. Increasing cellulase expression during the growth of *G. lucidum* G0119 coincides with results obtained in *Agaricus bisporus* and *Lentinula edodes* (30, 31). In the red and green modules, which are correlated with changes in cellulose content, one endoglucanase and one xylosidase are hub enzymes in each of modules. Degradation products such as glucose participate in carbohydrate catabolism, including the EMP, HMP, and TCA pathways. From the primordium to the young fruiting body phase, the EMP pathway is the primary catabolic pathway, consistent with results obtained previously for *Coprinus cinereus* (13).

In addition to carbohydrate catabolism, several carbohydrates were synthesized during growth. Trehalose, polyol, and polysaccharide contents increased from the mycelium growth phase to the primordium or young fruiting body phase but decreased from the mature fruiting body phase to the fully ejected spore phase. In previous research, the primary polysaccharides in *G. lucidum* were preliminarily concluded to be glycogen and β-glucan (27). The expression of metabolic enzymes also indicated that the levels of expression of glycogen and trehalose synthases generally increased in the first half of the growth cycle and deceased in the second half. In studies of *Flammulina*

FIG 6 Legend (Continued)
that were most positively and negatively correlated with genes in the corresponding modules. Correlation with *P* values lower than 0.05 are indicated by black asterisks. Abbreviations: U, upper layer of the substrate; M, middle layer of the substrate; L, lower layer of the substrate; P pileus; S, stipe; B, base; Lig, lignin; Cel, cellulose; Hemi, hemicellulose; Glc, glucose; Ara, arabinitol; Man, mannitol; Tre, trehalose; Pol, polysaccharide; GaC2, ganoderic acid C2; GraB, ganoderenic acid B; GaB, ganoderic acid B; GaA, ganoderic acid A; GaD, ganoderic acid D; GaF, ganoderic acid F; Gmt, ganodermanontriol; GaDM, ganoderic acid DM; GaS, ganoderic acid S; GaT, ganoderic acid T; GlB, ganoderiol B. (C) Hub genes and changes in their expression in each module are correlated with content changes.

velutipes and *C. cinereus*, glycogen and trehalose were also found to accumulate in the mycelium and in young fruiting bodies and to decrease after the fruiting bodies matured, consistent with the results in *G. lucidum* (32, 33).

Moreover, secondary metabolism, including triterpenoid synthesis, was initiated. Several synthases in the pathway upstream of triterpenoid synthesis, which involves catalysis of acetyl-CoA by ACAT, HMGR, and HMGS, were highly expressed, especially at P2 and P5. These enzymes in the MVA pathway have already been shown to increase the production of triterpenoids in *G. lucidum* (34–36). High expression of upstream enzymes could increase the synthesis of precursors and downstream products, including sterols and terpenoids. The pathway downstream of triterpenoid synthesis after the lanosterol step remains unclear. To date, there have been reports of regulation of triterpenoid synthesis through regulation of the expression of CYPs (19, 37), indicating that these enzymes might participate in certain steps downstream of triterpenoid synthesis. In the current study, seven CYPs were found to be coexpressed with LS, suggesting that they are correlated with the redox process after the lanosterol step. We found 1 CYP and 3 other CYPs that were positively correlated with changes in medium- and low-polarity triterpenoid contents, respectively. These compounds might be involved in downstream oxidation of the triterpenoid structure.

As acetyl-CoA can be obtained from carbohydrate or fat metabolism, the synthesis of triterpenoids could be correlated with the catabolism of carbohydrates. By increasing the synthesis of acetyl-CoA or adding intermediates of the TCA pathway or fat metabolism to *S. cerevisiae* and *Yarrowia lipolytica*, the production of the MVA by-product squalene could be increased (22, 38). A key enzyme in terpenoid upstream synthesis, deoxyxylulose 5-phosphate synthase, was also found to be correlated with transketolase from the HMP pathway and pyruvate dehydrogenase from the TCA pathway based on research in *Arabidopsis* (39). The formation of side chains in the triterpenoid skeleton was also found to be related to acetate in carbohydrate catabolism and to ribose in the HMP pathway in *Rhodopseudomonas* (40). In *G. lucidum*, ACAT, which catalyzes the synthesis of HMG-CoA from acetyl-CoA, was expressed at higher levels at P2 and P5, accompanied by increasing medium- and low-polarity triterpenoid contents. Taken together, these results suggest that the triterpenoid pathway is a branch of the carbohydrate pathway in fungi, plants and bacteria. An increase in carbohydrate catabolism could supply more precursors for the synthesis of triterpenoids in *G. lucidum*.

Additionally, the WGCNA data indicated that the expression of enzymes involved in triterpenoid synthesis, including phosphomevalonate kinase (MPK) and HMGR, is correlated with the expression of genes involved in cellulose degradation and the EMP and TCA pathways. Changes in triterpenoid content were also correlated with the expression of cellulase, hemicellulase, β-glucan synthase, and glycogen debranching enzyme. Changes in polyol and trehalose contents were correlated with the expression of cellulase, hemicellulase, β-glucan synthase, and HMP and TCA pathway enzymes. These correlations suggest that substrate degradation is connected to polysaccharide and triterpenoid synthesis through carbohydrate metabolism. This potential connection has been partially validated in several studies: when cell wall integrity and sporulation were inhibited, chitin and β-glucan contents decreased, and triterpenoid synthesis was also inhibited (41, 42). Additionally, the consumption of both HMP and polyol generates NADPH, which can increase the activity of HMGR and promote upstream triterpenoid synthesis (43).

During the last growth phase, when spores were produced at high levels and ejected, 21 lignocellulolytic enzymes were significantly upregulated. Several carbohydrates that had accumulated in the early phases decreased. Similarly, glycogen was found to decrease significantly in *C. cinereus* and *F. velutipes* when spores were produced, and a portion of the carbohydrates in spores were shown to be derived from the mycelium in the substrate (33, 44). This phenomenon may have occurred because the levels of the carbohydrates required to synthesize the structural components of spores increased markedly in this phase, as chitin and other carbohydrates account for

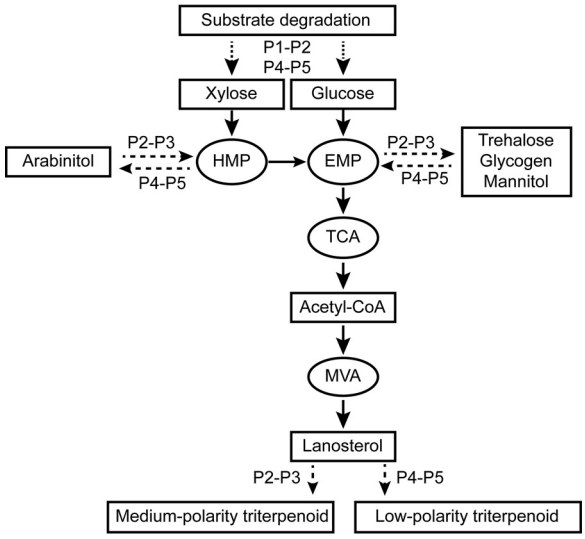

FIG 7 Potential correlation and changes in lignocellulose, carbohydrate, and triterpenoid levels during the growth of *G. lucidum*. In phases P1 and P2, lignocellulose is degraded into glucose and xylose, participates in carbohydrate catabolism, and is used to synthesize other carbohydrates, triggering the metabolism of triterpenoids. During P2 and P3, carbohydrate metabolism increases, and trehalose, glycogen, and polyol accumulate at high levels as the degradation of cellulose and hemicellulose increases. These changes provide more precursors for triterpenoid synthesis and increase the levels of medium-polarity triterpenoids. During P4 and P5, the production of many spores increases energy costs and generates a requirement for structural carbohydrate. Carbohydrate storage switches from anabolism to catabolism and, together with cellulose degradation, aids spore production. High levels of carbohydrate catabolism supply more precursors and increase the low-polarity triterpenoid content.

approximately 60 to 70% of the dry weight of spores (45). When the production of acetyl-CoA and ATP in the mitochondria of *Aspergillus flavus* was disrupted, spore germination was also inhibited, suggesting that the formation of spores is correlated with energy metabolism in fungi (46). Spore production by *G. lucidum* at this phase was much higher than that observed in other species. Such a large increase in metabolism requires an increased carbohydrate supply for energy and structural material. Therefore, the glycogen, trehalose, and mannitol contents decreased significantly at this phase. Additionally, the increased requirement for carbohydrate caused increased expression of lignocellulolytic enzymes, which then supplied more degradation products from the substrate.

In summary, substrate degradation during the growth of *G. lucidum* was found to be correlated with carbohydrate metabolism and triterpenoid synthesis, as illustrated in Fig. 7. From the mycelium growth phase to the primordium phase, along with the degradation of lignocellulose, degradation products enter carbohydrate metabolic pathways and are converted into multiple carbohydrates. Triterpenoid synthesis is then triggered by carbohydrate metabolism. From the primordium phase to the young fruiting body phase, cellulose and hemicellulose degradation increases, as does carbohydrate catabolism. Carbohydrates such as polyols, trehalose, and glycogen accumulate in storage. These changes stimulate the synthesis of medium-polarity triterpenoids. From the mature fruiting body phase to the spore ejection phase, at which time a very large number of spores are produced, more carbohydrates are required for energy and as structural components. Stored carbohydrates are consumed, and cellulose degradation also increases to meet this demand. The organism's highly regulated carbohydrate metabolism promotes an increase in the amount of low-polarity triterpenoids at this time. These correlations indicate that the synthesis of triterpenoids in *G. lucidum* could be enhanced not only by regulating the expression of enzymes in the triterpenoid pathway but also by regulating the expression of

enzymes involved in carbohydrate metabolism and substrate degradation. These findings suggest a practical way to regulate triterpenoid synthesis.

MATERIALS AND METHODS

Cultivation and sample collection. *G. lucidum* strain G0119 was obtained from the Institute of Edible Fungi at the Shanghai Academy of Agriculture Sciences, Shanghai, China. The strain was cultivated on a substrate containing 78% sawdust (maple, chestnut, and mulberry in a 1:1:1 ratio), 13% wheat bran, 7% corn flour, 1% sucrose, and 1% gypsum powder with 60% moisture content. Plastic bags (9 cm in diameter by 15 cm in height) were filled with the substrate, sterilized for 2 h at 120°C, and inoculated with strains grown on potato-dextrose agar medium. The bags were then incubated at 22 to 25°C for 1 to 2 months for mycelial growth. During development of the fruiting bodies, the temperature was maintained at 30 to 35°C, and the humidity was maintained at 80 to 95% by spraying with water for 5 min every 50 min.

The growth cycle was divided into 5 phases for sample testing: P1, fully grown mycelium (approximately 1 month after inoculation, when the mycelium had spread to the bottom of the substrate); P2, primordium (approximately 2 months after inoculation, when the primordium had formed a group of coral-like buttons); P3, young fruiting bodies (approximately 2.5 months after inoculation, when the pileus had formed on top of the stipe); P4, mature fruiting bodies (approximately 3.5 months after inoculation, when pore formation occurred and the pileus was fully extended); and P5, fully ejected spores (approximately 4.5 months after inoculation, when spores were ejected *en masse*). At each phase, samples were collected in triplicate from the substrate and fruiting bodies. Substrate samples were collected from the upper, middle, and lower layers of the substrate (each layer was 5 cm in height). Fruiting body samples were collected from the pileus, the stipe, and the base (the region between the stipe and the upper substrate layer). All of the collected samples were frozen in liquid nitrogen and preserved at −80°C. Samples for content determination were dried using an Alpha 2-4 LDplus freeze-dryer (Christ, Osterode, Germany) and ground using a DJ-10A grinder (Dianjiu, Shanghai, China) before testing.

Determination of the lignin, cellulose, and hemicellulose contents of the substrate. A modification of the Klason method was used to determine the lignin, cellulose, and hemicellulose contents of the substrate (47). Each ground sample (0.5 g of dry matter) was extracted with 10 ml of neutral washing solution (18.6 g/liter EDTA, 6.8 g/liter sodium borate, 30 g/liter lauryl sodium sulfate, 4.56 g/liter Na_2HPO_4, and 10 ml/liter glycol ether [pH 6.9 to 7.1]) at 100°C for 1 h to remove neutral soluble compounds. After centrifugation at 3,500 × *g* for 10 min, the supernatant was removed, and the pellet was dried using a freeze-dryer as described above and then hydrolyzed in 1 ml of 72% (wt/wt) H_2SO_4 at room temperature for 1 h. Next, 9 ml of distilled water was added to each sample, and the samples were hydrolyzed at 100°C for 3 h. After centrifugation as described above, the supernatant was collected for monosaccharide determination, and the pellet was dried at 105°C for 4 h. The lignin content was calculated based on the dry weight of the pellet minus the ash weight.

Monosaccharide concentrations were determined using an ICS5000+ HPAEC-PAD system (Thermo Scientific, CA, USA) equipped with a CarboPac PA20 column (150 by 3 mm; Dionex, CA, USA). The column temperature was 30°C, and the mobile phase was 2 mM NaOH at a flow rate of 0.40 ml/min. The external standard monosaccharides used were fucose, rhamnose, arabinose, galactose, glucose, mannose, xylose, and fructose (Sigma-Aldrich, MO, USA). The cellulose content was equal to the glucose content (wt/wt), with an anhydro correction of 0.9. The hemicellulose content was equal to the sum of the arabinose, galactose, mannose, and xylose contents (wt/wt) with anhydro corrections of 0.88 for xylose and arabinose and 0.9 for galactose and mannose (26, 48).

Determination of water-soluble carbohydrate and polysaccharide contents. Water-soluble carbohydrate levels were determined using an ICS2500 HPAEC-PAD system (Dionex, CA, USA) with a CarboPac MA1 column (250 by 4 mm; Dionex, CA, USA). The column temperature was 30°C, and the mobile phase was 480 mM sodium hydroxide at a flow rate of 0.40 ml/min. The external standards used were erythritol, fucose, trehalose, mannitol, arabinitol, mannose, glucose, galactose, and fructose (Sigma-Aldrich, MO, USA). Each sample (0.1 g of dry matter) was extracted with water for 2 h at 100°C. After centrifugation at 12,000 × *g* for 10 min, the supernatant was used for testing (28).

To obtain water-soluble polysaccharides, each sample (4 g of dry matter) was extracted with 200 ml of 80% ethanol by ultrasonic treatment (250 W, 40 kHz, three times for 30 min each) to remove low-molecular-weight carbohydrates. After vacuum filtration through filter paper, the residue was dried at 60°C, and water-soluble polysaccharides were extracted with 80 ml of water at 100°C for 2 h. The aqueous extract was filtered through filter paper and analyzed for total water-soluble polysaccharide content using the phenol-sulfuric acid method (27).

Determination of triterpenoid content. Triterpenoid levels were determined using a Waters 2695 HPLC system (Milford, MA, USA) equipped with a UV detector and an YMC ODS-AQ reversed-phase column (150 by 4.6 mm; YMC, Kyoto, Japan). The flow rate was 1.0 ml/min, and the column temperature was 30°C. The mobile phase consisted of 1% (vol/vol) acetic acid in Milli-Q water and methanol, and an isocratic program of 52% for 60 min and 48% for 30 min was used. The detection wavelength was 250 nm. The external standards used were ganoderic acid C2, ganoderic acid G, ganoderenic acid B, ganoderic acid B, ganoderic acid A, ganoderic acid D, ganoderic acid F, ganodermanontriol, ganoderic acid DM, ganoderic acid S, ganoderic acid T, and ganoderiol B. Each sample (0.1 g of dry matter) was extracted with 50 ml of 100% ethanol under ultrasonic treatment (250 W, 40 kHz) for 30 min. The suspension was filtered through 0.22-μm-pore nylon syringe filters and analyzed (27).

Expression of genes involved in lignocellulolytic degradation, carbohydrate metabolism, and triterpenoid metabolism. Genes involved in lignocellulose degradation, carbohydrate metabolism, and triterpenoid metabolism were selected from the *G. lucidum* G0119 genome based on their functional annotation. Gene expression was analyzed by transcriptome sequencing (RNA-seq) of the transcriptome. Total RNA was extracted from 0.1 mg of a sample from each growth phase using 1.5 ml of TRIzol reagent (Invitrogen, CA, USA); the extractions were performed in duplicate. RNA quantity and quality were determined using a Nanodrop spectrophotometer and agarose gel electrophoresis, respectively. cDNA library construction was performed according to the Illumina protocol. Sample libraries were sequenced using a HiSeq 3000 platform (Illumina, CA, USA). After filtering adapters and low-quality reads, clean raw reads from each growth phase were obtained and mapped to the *G. lucidum* G0119 genome (26). Gene expression levels were calculated by the fragments per kilobase per million (FPKM) method using RSEM with the default parameters. A heat map showing gene expression was generated using the statistical platform R with the package "pheatmap" (49). DEGs were identified using the DESeq package (50) by calculating $\log_2$ fold change (FPKM + 1). Fisher's test was used to calculate *P* values. Genes whose expression exhibited a fold change greater than 2 and a *P* value less than 0.05 were treated as DEGs.

Correlation and WGCNA. Correlation analysis of the lignocellulose, carbohydrate, and triterpenoid contents of samples from P2 to P5 was performed, as no data for the levels of these compounds in fruiting bodies at P1 were available. The analysis was performed using the statistical platform R project with the package "corrplot" (51). The Pearson method was used to calculate correlation coefficients.

WGCNA was used to create a topological overlap matrix by using the TOM similarity algorithm to summarize the associations among the expression levels of different genes. The matrix was created with the R project by installing the packages "WGCNA" (52, 53), "stringr" (54), and "reshape2" (55). The soft-thresholding power (β) used was 9, and the mergeCutHeight was 0.25. Genes were clustered into modules using the dynamic tree cutting method. The trait correlation between each module and each metabolite was calculated using weighted and Pearson correlation functions. Metabolites with correlation *P* values lower than 0.05 were deemed to be correlated with genes in their corresponding modules. For the genes in each module, a coexpression network was constructed using Cytoscape 3.7.0 (56). The "CytoHubba" app was used to evaluate the hub genes (57). The top 10 genes ranked by connection degree were selected as hub genes.

Data availability. Data from the *G. lucidum* G0119 genome are available in NCBI under BioProject accession no. PRJNA350580. Data from RNA sequencing of each growth phase are available in NCBI under Sequence Read Archive accession no. SRR6026942, SRR6027258, SRR6027261, SRR6027352, SRR6037451, SRR6037587, SRR6037726, SRR6040102, SRR6040213, and SRR6043945.

SUPPLEMENTAL MATERIAL

Supplemental material is available online only.

SUPPLEMENTAL FILE 1, PDF file, 0.9 MB.

SUPPLEMENTAL FILE 2, XLSX file, 0.02 MB.

SUPPLEMENTAL FILE 3, XLSX file, 0.02 MB.

ACKNOWLEDGMENTS

This research was supported by the Shanghai Agriculture Applied Technology Development Program of China (2018 no. 1-1), the Science and Technology Commission of Shanghai Municipality (19390743500), and the SAAS Program for Excellent Research Team (no. 2017A-06).

REFERENCES

1. Upton R, Graff A, Jolliffe G, Langer R, Williamson E. 2011. American herbal pharmacopoeia. CRC Press, Scotts Valley, CA.
2. Ulziijargal E, Mau J-L. 2011. Nutrient compositions of culinary-medicinal mushroom fruiting bodies and mycelia. Int J Med Mushrooms 13:343–349. https://doi.org/10.1615/IntJMedMushr.v13.i4.40.
3. Zhang J, Tang Q, Zimmerman-Kordmann M, Reutter W, Fan H. 2002. Activation of B lymphocytes by GLIS, a bioactive proteoglycan from *Ganoderma lucidum*. Life Sci 71:623–638. https://doi.org/10.1016/S0024-3205(02)01690-9.
4. Chang C, Lin C, Lu C, Martel J, Ko Y, Ojcius D, Tseng S, Wu T, Chen Y, Young J, Lai H. 2015. *Ganoderma lucidum* reduces obesity in mice by modulating the composition of the gut microbiota. Nat Commun 6:7489. https://doi.org/10.1038/ncomms8489.
5. Xu S, Dou Y, Ye B, Wu Q, Wang Y, Hu M, Ma F, Rong X, Guo J. 2017. *Ganoderma lucidum* polysaccharides improve insulin sensitivity by regulating inflammatory cytokines and gut microbiota composition in mice. J Funct Foods 38:545–552. https://doi.org/10.1016/j.jff.2017.09.032.
6. Yue Q-X, Song X-Y, Ma C, Feng L-X, Guan S-H, Wu W-Y, Yang M, Jiang B-H, Liu X, Cui Y-J, Guo D-A. 2010. Effects of triterpenes from *Ganoderma lucidum* on protein expression profile of HeLa cells. Phytomedicine 17:606–613. https://doi.org/10.1016/j.phymed.2009.12.013.
7. Wu GS, Lu JJ, Guo JJ, Li YB, Tan W, Dang YY, Zhong ZF, Xu ZT, Chen XP, Wang YT. 2012. Ganoderic acid DM, a natural triterpenoid, induces DNA damage, G_1 cell cycle arrest and apoptosis in human breast cancer cells. Fitoterapia 83:408–414. https://doi.org/10.1016/j.fitote.2011.12.004.
8. Wu H, Tang S, Huang Z, Zhou Q, Zhang P, Chen Z. 2016. Hepatoprotective effects and mechanisms of action of triterpenoids from Lingzhi or Reishi medicinal mushroom *Ganoderma lucidum* (Agaricomycetes) on alpha-amanitin-induced liver injury in mice. Int J Med Mushrooms 18:841–850. https://doi.org/10.1615/IntJMedMushrooms.v18.i9.80.
9. Akihisa T, Nakamura Y, Tagata M, Tokuda H, Yasukawa K, Uchiyama E, Suzuki T, Kimura Y. 2007. Anti-inflammatory and anti-tumor-promoting effects of triterpene acids and sterols from the fungus *Ganoderma lucidum*. Chem Biodivers 4:224–231. https://doi.org/10.1002/cbdv.200790027.
10. Janusz G, Kucharzyk KH, Pawlik A, Staszczak M, Paszczynski AJ. 2013. Fungal laccase, manganese peroxidase and lignin peroxidase: gene expression and regulation. Enzyme Microb Technol 52:1–12. https://doi.org/10.1016/j.enzmictec.2012.10.003.

11. Shoham Y, Lamed R, Bayer EA. 1999. The cellulosome concept as an efficient microbial strategy for the degradation of insoluble polysaccharides. Trends Microbiol 7:275–281. https://doi.org/10.1016/S0966-842X(99)01533-4.
12. Martínez ÁT, Speranza M, Ruiz-Dueñas FJ, Ferreira P, Camarero S, Guillén F, Martínez MJ, Gutiérrez A, del Río JC. 2010. Biodegradation of lignocellulosics: microbial, chemical, and enzymatic aspects of the fungal attack of lignin. Int Microbiol 8:195–204.
13. Moore D, Ewaze JO. 1976. Activities of some enzymes involved in metabolism of carbohydrate during sporophore development in *Coprinus cinereus*. Microbiology 97:313–322. https://doi.org/10.1099/00221287-97-2-313.
14. Hammond J, Nichols R. 1977. Carbohydrate metabolism in *Agaricus bisporus* (Lange) Imbach.: metabolism of [^{14}C] labelled sugars by sporophores and mycelium. New Phytol 79:315–325. https://doi.org/10.1111/j.1469-8137.1977.tb02211.x.
15. Kitamoto Y, Kobayashi J, Ichikawa Y. 1981. Carbohydrate metabolism in fruit-body formation of Flammulina velutipes, abstr 519. Abstr Annu Meet Agric Chem Soc Japan.
16. Latge JP. 2007. The cell wall: a carbohydrate armour for the fungal cell. Mol Microbiol 66:279–290. https://doi.org/10.1111/j.1365-2958.2007.05872.x.
17. Bidochka MJ, Low NH, Khachatourians GG. 1990. Carbohydrate storage in the entomopathogenic fungus *Beauveria bassiana*. Appl Environ Microbiol 56:3186–3190. https://doi.org/10.1128/AEM.56.10.3186-3190.1990.
18. Liu D, Gong J, Dai W, Kang X, Huang Z, Zhang HM, Liu W, Liu L, Ma J, Xia Z, Chen Y, Chen Y, Wang D, Ni P, Guo AY, Xiong X. 2012. The genome of *Ganoderma lucidum* provides insights into triterpenes biosynthesis and wood degradation. PLoS One 7:e36146. https://doi.org/10.1371/journal.pone.0036146.
19. Yang C, Li W, Li C, Zhou Z, Xiao Y, Yan X. 2018. Metabolism of ganoderic acids by a *Ganoderma lucidum* cytochrome P450 and the 3-keto sterol reductase ERG27 from yeast. Phytochemistry 155:83–92. https://doi.org/10.1016/j.phytochem.2018.07.009.
20. Xiao H, Zhang Y, Wang M. 2018. Discovery and engineering of cytochrome P450s for terpenoid biosynthesis. Trends Biotechnol 37:678–681. https://doi.org/10.1016/j.tibtech.2018.11.008.
21. Ma L, Chen L, Zhang L, Zou G, Liu R, Jiang Y, Zhou Z. 2016. RNA sequencing reveals Xyr1 as a transcription factor regulating gene expression beyond carbohydrate metabolism. Biomed Res Int 2016:4841756. https://doi.org/10.1155/2016/4841756.
22. Wei LJ, Kwak S, Liu JJ, Lane S, Hua Q, Kweon DH, Jin YS. 2018. Improved squalene production through increasing lipid contents in *Saccharomyces cerevisiae*. Biotechnol Bioeng 115:1793–1800. https://doi.org/10.1002/bit.26595.
23. Yu G, Yin Y, Yu W, Liu W, Jin Y, Shrestha A, Yang Q, Ye X, Sun H. 2015. Proteome exploration to provide a resource for the investigation of *Ganoderma lucidum*. PLoS One 10:e0119439. https://doi.org/10.1371/journal.pone.0119439.
24. Chen S, Xu J, Liu C, Zhu Y, Nelson DR, Zhou S, Li C, Wang L, Guo X, Sun Y, Luo H, Li Y, Song J, Henrissat B, Levasseur A, Qian J, Li J, Luo X, Shi L, He L, Xiang L, Xu X, Niu Y, Li Q, Han MV, Yan H, Zhang J, Chen H, Lv A, Wang Z, Liu M, Schwartz DC, Sun C. 2012. Genome sequence of the model medicinal mushroom *Ganoderma lucidum*. Nat Commun 3:913. https://doi.org/10.1038/ncomms1923.
25. Nakagawa T, Zhu Q, Tamrakar S, Amen Y, Mori Y, Suhara H, Kaneko S, Kawashima H, Okuzono K, Inoue Y, Ohnuki K, Shimizu K. 2018. Changes in content of triterpenoids and polysaccharides in *Ganoderma lingzhi* at different growth stages. J Nat Med 72:734–744. https://doi.org/10.1007/s11418-018-1213-y.
26. Zhou S, Zhang J, Ma F, Tang C, Tang Q, Zhang X. 2018. Investigation of lignocellulolytic enzymes during different growth phases of *Ganoderma lucidum* strain G0119 using genomic, transcriptomic and secretomic analyses. PLoS One 13:e0198404. https://doi.org/10.1371/journal.pone.0198404.
27. Zhou S, Tang Q, Tang C, Liu Y, Ma F, Zhang X, Zhang J. 2018. Triterpenes and soluble polysaccharide changes in Lingzhi or Reishi medicinal mushroom, *Ganoderma lucidum* (Agaricomycetes), during fruiting growth. Int J Med Mushrooms 20:859–871. https://doi.org/10.1615/IntJMedMushrooms.2018027357.
28. Zhou S, Zhang X, Tang C, Ma F, Tang Q, Zhang J. 2018. Change of polyol and trehalose content and expression of their related metabolism enzymes in *Ganoderma lingzhi* SH during fruiting body growth. Mycosystema 37:1090–1099.
29. Kubicek CP. 2013. Fungi and lignocellulosic biomass. Wiley-Blackwell, Ames, IA.
30. Pontes MVA, Patyshakuliyeva A, Post H, Jurak E, Hilden K, Altelaar M, Heck A, Kabel MA, de Vries RP, Makela MR. 2018. The physiology of *Agaricus bisporus* in semi-commercial compost cultivation appears to be highly conserved among unrelated isolates. Fungal Genet Biol 112:12–20. https://doi.org/10.1016/j.fgb.2017.12.004.
31. Ohga S, Royse D. 2001. Transcriptional regulation of laccase and cellulase genes during growth and fruiting of *Lentinula edodes* on supplemented sawdust. FEMS Microbiol Lett 201:111–115. https://doi.org/10.1111/j.1574-6968.2001.tb10741.x.
32. Kitamoto Y, Kobayashi A, Mori N, Ohga S. 2001. Metabolic function of glycogen phosphorylase and trehalose phosphorylase in fruit-body formation of *Flammulina velutipes*. Mycoscience 42:143–147. https://doi.org/10.1007/BF02464130.
33. Ji J, Moore D. 1993. Glycogen metabolism in relation to fruit body maturation in *Coprinus cinereus*. Mycol Res 97:283–289. https://doi.org/10.1016/S0953-7562(09)81121-0.
34. Hu Y, Li M, Wang S, Yue S, Shi L, Ren A, Zhao M. 2018. *Ganoderma lucidum* phosphoglucomutase is required for hyphal growth, polysaccharide production, and cell wall integrity. Appl Microbiol Biotechnol 102:1911–1922. https://doi.org/10.1007/s00253-017-8730-6.
35. Xu JW, Xu YN, Zhong JJ. 2010. Production of individual ganoderic acids and expression of biosynthetic genes in liquid static and shaking cultures of *Ganoderma lucidum*. Appl Microbiol Biotechnol 85:941–948. https://doi.org/10.1007/s00253-009-2106-5.
36. Shi L, Qin L, Xu Y, Ren A, Fang X, Mu D, Tan Q, Zhao M. 2012. Molecular cloning, characterization, and function analysis of a mevalonate pyrophosphate decarboxylase gene from *Ganoderma lucidum*. Mol Biol Rep 39:6149–6159. https://doi.org/10.1007/s11033-011-1431-9.
37. Lan X, Yuan W, Wang M, Xiao H. 2019. Efficient biosynthesis of antitumor ganoderic acid HLDOA using a dual tunable system for optimizing the expression of CYP5150L8 and a *Ganoderma* P450 reductase. Biotechnol Bioeng 116:3301–3311. https://doi.org/10.1002/bit.27154.
38. Huang YY, Jian XX, Lv YB, Nian KQ, Gao Q, Chen J, Wei LJ, Hua Q. 2018. Enhanced squalene biosynthesis in *Yarrowia lipolytica* based on metabolically engineered acetyl-CoA metabolism. J Biotechnol 281:106–114. https://doi.org/10.1016/j.jbiotec.2018.07.001.
39. Wright LP, Rohwer JM, Ghirardo A, Hammerbacher A, Ortiz-Alcaide M, Raguschke B, Schnitzler J-P, Gershenzon J, Phillips MA. 2014. Deoxyxylulose 5-phosphate synthase controls flux through the methylerythritol 4-phosphate pathway in *Arabidopsis*. Plant Physiol 165:1488–1504. https://doi.org/10.1104/pp.114.245191.
40. Flesch G, Rohmer M. 1988. Prokaryotic hopanoids: the biosynthesis of the bacteriohopane skeleton. Eur J Biochem 175:405–411. https://doi.org/10.1111/j.1432-1033.1988.tb14210.x.
41. Zhang G, Sun Z, Ren A, Shi L, Shi D, Li X, Zhao M. 2017. The mitogen-activated protein kinase GlSlt2 regulates fungal growth, fruiting body development, cell wall integrity, oxidative stress and ganoderic acid biosynthesis in *Ganoderma lucidum*. Fungal Genet Biol 104:6–15. https://doi.org/10.1016/j.fgb.2017.04.004.
42. Wang S, Shi L, Hu Y, Liu R, Ren A, Zhu J, Zhao M. 2018. Roles of the Skn7 response regulator in stress resistance, cell wall integrity and GA biosynthesis in *Ganoderma lucidum*. Fungal Genet Biol 114:12–23. https://doi.org/10.1016/j.fgb.2018.03.002.
43. Paramasivan K, Mutturi S. 2017. Regeneration of NADPH coupled with HMG-CoA reductase activity increases squalene synthesis in *Saccharomyces cerevisiae*. J Agric Food Chem 65:8162–8170. https://doi.org/10.1021/acs.jafc.7b02945.
44. Kitamoto Y, Kikuchi A, Mori N, Ohga S. 2000. Polyol metabolism in the mycelium and fruit-bodies during development of *Flammulina velutipes*. Mycoscience 41:461–465. https://doi.org/10.1007/BF02461665.
45. Chen T, Li K, Xu J, Zhu P, Zhen Y. 1997. Study on log-cultivated *Ganoderma lucidum* spores. (II) General properties and chemical components. Acta Edulis Fungi 4:22–26.
46. Ma W, Zhao L, Zhao W, Xie Y. 2019. (E)-2-Hexenal, as a potential natural antifungal compound, inhibits *Aspergillus flavus* spore germination by disrupting mitochondrial energy metabolism. J Agric Food Chem 67:1138–1145. https://doi.org/10.1021/acs.jafc.8b06367.
47. Jurak E, Punt AM, Arts W, Kabel MA, Gruppen H. 2015. Fate of carbohydrates and lignin during composting and mycelium growth of *Agaricus bisporus* on wheat straw based compost. PLoS One 10:e0138909. https://doi.org/10.1371/journal.pone.0138909.
48. Sluiter A, Hames B, Ruiz R, Scarlata C, Sluiter J, Templeton D, Crocker D. 2008. Determination of structural carbohydrates and 1ignin in biomass. Laboratory analytical procedure. National Renewable Energy Laboratory, Golden, CO.

49. Raivo K. 2019. pheatmap: pretty heatmaps. R package version 1.0.12. https://CRAN.R-project.org/package=pheatmap.
50. Anders S, Huber W. 2010. Differential expression analysis for sequence count data. Genome Biol 11:R106. https://doi.org/10.1186/gb-2010-11-10-r106.
51. Taiyun W, Viliam S. 2017. R package "corrplot": visualization of a correlation matrix (version 0.84). https://github.com/taiyun/corrplot.
52. Langfelder P, Horvath S. 2008. WGCNA: an R package for weighted correlation network analysis. BMC Bioinformatics 9:559. https://doi.org/10.1186/1471-2105-9-559.
53. Langfelder P, Horvath S. 2012. Fast R functions for robust correlations and hierarchical clustering. J Stat Softw 46:i11.
54. Hadley W. 2019. stringr: simple, consistent wrappers for common string operations. R package version 1.4.0. https://CRAN.R-project.org/package=stringr.
55. Hadley W. 2007. Reshaping data with the reshape package. J Stat Softw 21:1–20. https://doi.org/10.18637/jss.v021.i12.
56. Shannon P, Markiel A, Ozier O, Baliga NS, Wang JT, Ramage D, Amin N, Schwikowski B, Ideker T. 2003. Cytoscape: a software environment for integrated models of biomolecular interaction networks. Genome Res 13:2498–2504. https://doi.org/10.1101/gr.1239303.
57. Chin CH, Chen SH, Wu HH, Ho CW, Ko MT, Lin CY. 2014. cytoHubba: identifying hub objects and sub-networks from complex interactome. BMC Syst Biol 8:S11. https://doi.org/10.1186/1752-0509-8-S4-S11.